



Available online at <http://scik.org>

Commun. Math. Biol. Neurosci. 2020, 2020:71

<https://doi.org/10.28919/cmbn/4990>

ISSN: 2052-2541

## THE HIDDEN ROLE OF THE PRE-SYMPTOMATIC INDIVIDUALS IN THE TRANSMISSION DYNAMICS OF COVID-19

NASSER AL-SALTI<sup>1</sup>, FATMA AL-MUSALHI<sup>2,\*</sup>, MARYAM AL-YAHYAI<sup>1</sup>, IBRAHIM M. ELMOJTABA<sup>1</sup>

<sup>1</sup>Department of Mathematics, Sultan Qaboos University, Al-Khoudh 123, Oman

<sup>2</sup>Center for Preparatory Studies, Sultan Qaboos University, Al-Khoudh 123, Oman

Copyright © 2020 the author(s). This is an open access article distributed under the Creative Commons Attribution License, which permits unrestricted use, distribution, and reproduction in any medium, provided the original work is properly cited.

**Abstract.** In this paper, a mathematical model with four different routes of transmission, namely, asymptomatic, pre-symptomatic, symptomatic and environmental transmissions, has been proposed and analyzed to investigate the role of pre-symptomatic individuals in the transmission dynamics of COVID-19 outbreak. Using the next generation matrix method, the basic reproduction number  $R_0$  has been derived and then sensitivity analysis of the proposed model is presented. Existence and stability analysis of disease free and endemic equilibrium points have been discussed. Numerical simulations to demonstrate the effect of some model parameters related to pre-symptomatic transmission on the disease transmission dynamics have been carried out.

**Keywords:** COVID-19; pre-symptomatic individuals; basic reproduction number; stability analysis; sensitivity analysis.

**2010 AMS Subject Classification:** 34C23, 34D23, 92D30.

### 1. INTRODUCTION

COVID-19 outbreak has spread rapidly and has infected more than 21 millions and caused more than 700 thousands death cases worldwide by August 17, 2020. Due to the widespread

---

\*Corresponding author

E-mail address: [fatma@squ.edu.om](mailto:fatma@squ.edu.om)

Received September 2, 2020

transmission, scientists and medical experts accelerate their work to develop an effective vaccine for such highly contagious infection. Recently, a number of countries have reported development in COVID-19 vaccine trials and some vaccines entered the clinical trials [13]. However, even if approved vaccination is available, it might be expensive and hence it might not be available to all countries.

The transmission, symptoms, diagnosis and mathematical models will provide important references for the researchers toward the ongoing development of vaccines and also controlling the spread of this disease [13]. Moreover, understanding the virus transmission and its clinical characteristics are very important and would be helpful in building an appropriate mathematical model.

Furthermore, the time when the person become infectious played a crucial role in the fast spread of the virus globally. According to the WHO report, there are evidences on transmission from asymptomatic (infectious but never show symptoms) and pre-symptomatic individuals (infectious but shows symptoms later), see [7, 10, 23, 25], this implies that if the person have the virus but did not show any symptoms he could infect others before symptom onset and in some cases will not develop any symptoms later. When the incubation period is longer than latency period this may lead to the occurrence of pre-symptomatic transmission, see [9, 10, 12, 15, 22] and some empirical studies have indicted that the peak of infectious period occurred before symptom onset during pre-symptomatic period [9, 22, 25].

The silent infections due to pre-symptomatic and asymptomatic transmissions have critical contribution to the quick spread of the disease and this will further reduce the effectiveness of control measures which focus on symptomatic people such isolation and using face masks for symptomatic people. Therefore, the control strategies should be extended to pre-symptomatic and asymptomatic individuals. A rapid, systematic testing and contact tracing are needed to detect these cases and more restrictions should be implemented to minimize the risk of the silent transmissions.

Epidemiological models provide useful guidelines to inform policy making and outbreak management and also powerful for exploring different scenarios [21]. Several epidemic models have been considered to study the spread of COVID19 and investigate the transmission of

asymptomatic, symptomatic and also environmental transmissions, see for example [1, 5, 14, 16, 18, 24]. But, few studies take into account the effect of pre-symptomatic transmission, see for example [8], which has an important role in the spread of the disease as mentioned above. Here, we assume four routes of transmissions: pre-symptomatic, asymptomatic, symptomatic and environmental and investigate the role of pre-symptomatic transmission. The rest of the paper is organized as follows. In the next section, we present the proposed mathematical model. The mathematical analysis of the proposed model will be carried out in Section 3. The analysis includes invariant region, the calculations of the basic reproduction number, sensitivity analysis and stability analysis. In Section 4, numerical simulations are carried out to illustrate the effect of some model parameters related to the pre-symptomatic transmission. Finally, a brief conclusion is presented in Section 5.

## 2. MATHEMATICAL MODEL FORMULATION

Here, we give a description of the proposed model. It is observed that COVID19 can be transmitted directly via droplets and close contact with infected people and indirectly via contaminated surfaces. The human population is divided into six classes; susceptible class  $\tilde{S}(t)$ , exposed class  $\tilde{E}(t)$ , asymptomatic class  $\tilde{A}(t)$ , pre-symptomatic class  $\tilde{P}(t)$ , symptomatic class  $\tilde{I}(t)$ , and recovered class  $\tilde{R}(t)$ , so that  $\tilde{N}(t) = \tilde{S}(t) + \tilde{E}(t) + \tilde{A}(t) + \tilde{P}(t) + \tilde{I}(t) + \tilde{R}(t)$ . The asymptomatic and pre-symptomatic individuals can transmit the virus even though they don't show symptoms. The difference between these two classes is that pre-symptomatic will later develop symptoms and enter the symptomatic class, whereas asymptomatic individuals will never show symptoms till they recover. Thus, we assume that the exposed class (latently infected but still not infectious) enter contagious classes at different rates; asymptomatic at a rate  $\lambda_1$ , pre-symptomatic at a rate  $\lambda_2$  and symptomatic at a rate  $\lambda_3$  depending on symptoms and contagiousness. Here, we assume that some infected individuals become infectious before developing symptoms and the rest will only be infectious after developing symptoms [23].

For indirect transmission, we assume  $\frac{\beta_e \tilde{B}}{k + \tilde{B}}$  to be the force of infection related to contaminated environment, where  $\tilde{B}$  represents the concentration of the virus in the environment and  $\beta_e$  is the contact rate with the contaminated environment. The expression  $\frac{\tilde{B}}{k + \tilde{B}}$  represents the probability of catching the disease and the constant  $k$  represents the minimum concentration of virus at

environment capable of ensuring 50% chance of contracting the disease. The model diagram is illustrated in Figure 1.

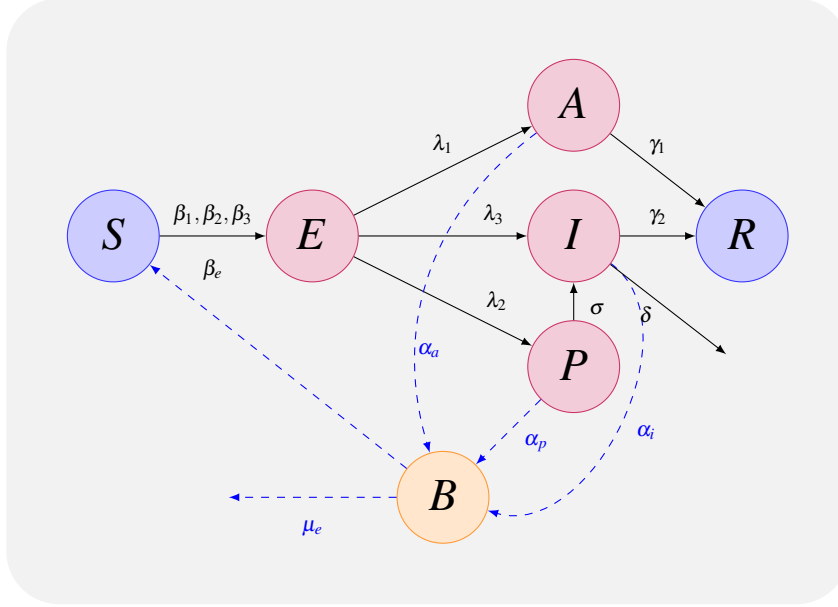


FIGURE 1. Transmission diagram of the model

In [9], it was shown that the peak of infectiousness occurs at 0-2 days before symptoms onset. So, we assume that the pre-symptomatic individuals are more contagious and their shedding rate  $\alpha_p$  is higher than the shedding rates of symptomatic  $\alpha_i$  and asymptomatic  $\alpha_a$ . All parameters are defined in table 1. The proposed mathematical model is given by the following set of equations:

$$\begin{aligned}
 \tilde{S}' &= \Lambda - \beta_1 \tilde{A} \frac{\tilde{S}}{\tilde{N}} - \beta_2 \tilde{P} \frac{\tilde{S}}{\tilde{N}} - \beta_3 \tilde{I} \frac{\tilde{S}}{\tilde{N}} - \frac{\beta_e \tilde{B} \tilde{S}}{k + \tilde{B}} - \mu \tilde{S} \\
 \tilde{E}' &= \beta_1 \tilde{A} \frac{\tilde{S}}{\tilde{N}} + \beta_2 \tilde{P} \frac{\tilde{S}}{\tilde{N}} + \beta_3 \tilde{I} \frac{\tilde{S}}{\tilde{N}} + \frac{\beta_e \tilde{B} \tilde{S}}{k + \tilde{B}} - (\mu + \lambda_1 + \lambda_2 + \lambda_3) \tilde{E} \\
 \tilde{A}' &= \lambda_1 \tilde{E} - (\mu + \gamma_1) \tilde{A} \\
 \tilde{P}' &= \lambda_2 \tilde{E} - (\mu + \sigma) \tilde{P} \\
 \tilde{I}' &= \lambda_3 \tilde{E} + \sigma \tilde{P} - (\mu + \gamma_2 + \delta) \tilde{I} \\
 \tilde{R}' &= \gamma_1 \tilde{A} + \gamma_2 \tilde{I} - \mu \tilde{R} \\
 \tilde{B}' &= \alpha_a \tilde{A} + \alpha_p \tilde{P} + \alpha_i \tilde{I} - \mu_e \tilde{B}.
 \end{aligned}
 \tag{1}$$

Here  $\tilde{N}'(t) = \Lambda - \mu\tilde{N} - \delta\tilde{I}$ .

TABLE 1. Parameters used in model (1)

Parameter	Symbol	Value [ref.]
Natural death/birth rate	$\mu$	0.000033 assumed
Disease related death rate of humans	$\delta$	0.04 [8]
Recruitment Rate	$\Lambda$	
Contact rate with contaminated environment	$\beta_e$	0.0414 [14]
Shedding rate from asymptomatic to environment	$\alpha_a$	0.05 [14]
Shedding rate from pre-symptomatic to environment	$\alpha_p$	0.1 assumed
Shedding rate from symptomatic to environment	$\alpha_i$	0.07 assumed
Life time of the virus in the environment	$1/\mu_e$	5.8 [14]
Transmission rate of the disease from asymptomatic	$\beta_1$	0.125 [8]
Transmission rate of the disease from pre-symptomatic	$\beta_2$	3.7875 [8]
Transmission rate of the disease from symptomatic	$\beta_3$	0.12875 [8]
Rate at which exposed become asymptomatic	$\lambda_1$	0.3128[11],[8]
Rate at which exposed become pre-symptomatic	$\lambda_2$	0.0898 [11],[8]
Rate at which exposed become symptomatic	$\lambda_3$	0.0553 [11],[8]
Rate at which pre-symptomatic become symptomatic	$\sigma$	0.5 [9]
Recovery rate of asymptomatic individuals	$\gamma_1$	0.1397 [8]
Recovery rate of symptomatic individuals	$\gamma_2$	0.0698 [8]

The parameters  $\lambda_1$ ,  $\lambda_2$ , and  $\lambda_3$  can be written in general as follows

$$\lambda_1 = \frac{1}{3.2}\varepsilon_1, \quad \lambda_2 = \frac{1}{3.2}\varepsilon_2(1 - \varepsilon_1), \quad \lambda_3 = \frac{1}{5.2} * (1 - \varepsilon_1)(1 - \varepsilon_2),$$

where, the incubation period and infectious period before symptom onset are taken to be 5.2 and 2 days, respectively, as in [9]. Here,  $\varepsilon_1$  represents the proportion of asymptomatic infections and according to [11] the confirmed asymptomatic infections represents 42.5% of the total infections, so the remaining will eventually develop symptoms. In table 1, it is taken  $\varepsilon_1 = 0.425$ .

Moreover,  $\varepsilon_2$  represents the proportion of pre-symptomatic individuals, which is taken to be  $\varepsilon_2 = 0.5$ .

### 3. MATHEMATICAL ANALYSIS OF THE MODEL

**3.1. Normalized Model.** Let us define the following

$$N = \frac{\tilde{N}}{\mathcal{N}}, \quad S = \frac{\tilde{S}}{\mathcal{N}}, \quad E = \frac{\tilde{E}}{\mathcal{N}}, \quad A = \frac{\tilde{A}}{\mathcal{N}},$$

$$P = \frac{\tilde{P}}{\mathcal{N}}, \quad I = \frac{\tilde{I}}{\mathcal{N}}, \quad R = \frac{\tilde{R}}{\mathcal{N}}, \quad B = \frac{\tilde{B}}{\mathcal{B}},$$

where  $\mathcal{N} = \Lambda/\mu$  and  $\mathcal{B} = (\alpha_p\Lambda)/(\mu_e\mu)$ . Then, model (1) can be written in normalized form as follows:

$$\begin{aligned} S' &= \mu - \beta_1 A \frac{S}{N} - \beta_2 P \frac{S}{N} - \beta_3 I \frac{S}{N} - \frac{\beta_e BS}{K+B} - \mu S \\ E' &= \beta_1 A \frac{S}{N} + \beta_2 P \frac{S}{N} + \beta_3 I \frac{S}{N} + \frac{\beta_e BS}{K+B} - (\mu + \lambda_1 + \lambda_2 + \lambda_3) E \\ A' &= \lambda_1 E - (\mu + \gamma_1) A \\ P' &= \lambda_2 E - (\mu + \sigma) P \\ I' &= \lambda_3 E + \sigma P - (\mu + \gamma_2 + \delta) I \\ R' &= \gamma_1 A + \gamma_2 I - \mu R \\ B' &= \alpha_1 \mu_e A + \mu_e P + \alpha_2 \mu_e I - \mu_e B \end{aligned} \tag{2}$$

where  $\alpha_1 = \frac{\alpha_a}{\alpha_p}$ ,  $\alpha_2 = \frac{\alpha_i}{\alpha_p}$  and  $K = \frac{k}{(\alpha_p\Lambda)/(\mu_e\mu)}$ .

**3.2. Invariant region.** Model (2) will be analyzed in a bounded feasible-biological region.

We first, note that the total population  $N(t)$  satisfies

$$N'(t) = \mu - \mu N - \delta I(t) \leq \mu - \mu N.$$

Then, it can be shown that

$$N(t) \leq (N(0) - 1)e^{-\mu t} + 1.$$

which implies that  $N(t) \leq 1$ . Similarly, for  $B$  we have

$$B' = \alpha_1 \mu_e A + \mu_e P + \alpha_2 \mu_e I - \mu_e B \leq \mu_e N - \mu_e B \leq \mu_e - \mu_e B.$$

Thus,  $B$  satisfies the following inequality

$$B \leq (B(0) - 1)e^{-\mu_e t} + 1,$$

which implies  $B(t) \leq 1$ . Hence, we have the following bounded positive invariant set

$$\Omega = \{(S, E, A, P, I, R, B) \in \mathbb{R}_+^7 : 0 < S + E + A + P + I + R \leq 1, 0 < B \leq 1\}.$$

**3.3. The basic reproduction number.** The disease free equilibrium (DFE) of the model is given by  $E_0 = (1, 0, 0, 0, 0, 0, 0)$ . Then, using the next generation method, we calculate  $R_0$  as follows:

the matrix of new infection is

$$\mathcal{F} = \begin{bmatrix} \beta_1 A \frac{S}{N} + \beta_2 P \frac{S}{N} + \beta_3 I \frac{S}{N} + \frac{\beta_e B S}{K+B} \\ 0 \\ 0 \\ 0 \\ 0 \end{bmatrix}$$

and the matrix of transition terms is

$$\mathcal{V} = \begin{bmatrix} \xi E \\ -\lambda_1 E + (\mu + \gamma_1) A \\ -\lambda_2 E + (\mu + \sigma) P \\ -\lambda_3 E - \sigma P + \eta I \\ -\alpha_1 \mu_e A - \mu_e P - \alpha_2 \mu_e I + \mu_e B \end{bmatrix},$$

where  $\xi = (\mu + \lambda_1 + \lambda_2 + \lambda_3)$  and  $\eta = (\mu + \gamma_2 + \delta)$ . Then, the Jacobian of  $\mathcal{F}$  at  $E_0$  denoted by  $F$  is given by

$$(3) \quad F = \begin{bmatrix} 0 & \beta_1 & \beta_2 & \beta_3 & \frac{\beta_e}{K} \\ 0 & 0 & 0 & 0 & 0 \\ 0 & 0 & 0 & 0 & 0 \\ 0 & 0 & 0 & 0 & 0 \\ 0 & 0 & 0 & 0 & 0 \end{bmatrix}$$

and the Jacobian of  $\mathcal{V}$  at  $E_0$  denoted by  $V$  is given by

$$(4) \quad V = \begin{bmatrix} \xi & 0 & 0 & 0 & 0 \\ -\lambda_1 & \mu + \gamma_1 & 0 & 0 & 0 \\ -\lambda_2 & 0 & \mu + \sigma & 0 & 0 \\ -\lambda_3 & 0 & -\sigma & \eta & 0 \\ 0 & -\alpha_1 \mu_e & -\mu_e & -\alpha_2 \mu_e & \mu_e \end{bmatrix}.$$

Hence, the next generation matrix is

$$FV^{-1} = \begin{bmatrix} R_{hh} + R_{he} & \frac{\beta_1}{\mu + \gamma_1} + \frac{\beta_e \alpha_1}{K(\mu + \gamma_1)} & \frac{\beta_2}{(\mu + \sigma)} + \frac{\beta_3 \sigma}{(\mu + \sigma)\eta} + \frac{\beta_e(\eta + \alpha_2 \sigma)}{K\eta(\mu + \sigma)} & \frac{\beta_3}{\eta} + \frac{\beta_e \alpha_2}{K\eta} & \frac{\beta_e}{K\mu_e} \\ 0 & 0 & 0 & 0 & 0 \\ 0 & 0 & 0 & 0 & 0 \\ 0 & 0 & 0 & 0 & 0 \\ 0 & 0 & 0 & 0 & 0 \end{bmatrix},$$

where  $R_{hh}$  can be written as

$$R_{hh} = R_a + R_p + R_i,$$

with

$$R_a = \frac{\beta_1 \lambda_1}{\xi(\mu + \gamma_1)}, \quad R_p = \frac{\beta_2 \lambda_2}{\xi(\mu + \sigma)}, \quad R_i = \frac{\beta_3(\lambda_2 \sigma + \lambda_3(\mu + \sigma))}{\xi \eta(\mu + \sigma)}.$$

Similarly,  $R_{he}$  can be written as

$$R_{he} = R_{ae} + R_{pe} + R_{ie},$$

where

$$R_{ae} = \frac{\beta_e \lambda_1 \alpha_1}{K \xi(\mu + \gamma_1)}, \quad R_{pe} = \frac{\beta_e \lambda_2}{K \xi(\mu + \sigma)}, \quad R_{ie} = \frac{\beta_e \alpha_2(\lambda_2 \sigma + \lambda_3(\mu + \sigma))}{K \xi \eta(\mu + \sigma)}.$$

Thus, the basic reproduction number is the spectral radius of the next generation matrix  $FV^{-1}$  and it is given by

$$R_0 = R_{hh} + R_{he}.$$

It is clear that  $R_{hh}$  gives the contribution from human to human transmission and  $R_{he}$  gives the contribution from environment to human transmission. Moreover, each expression includes three parts, which correspond to asymptomatic, pre-symptomatic and symptomatic transmissions, respectively. The basic reproduction number is the sum of all these contributions. If any



of them is greater than one, then the basic reproduction number  $R_0 > 1$ . This emphasizes the fact that to reduce the spread of COVID19, all transmission routes must be controlled.

Note that in the above calculations, the term  $\alpha_1\mu_eA + \mu_eP + \alpha_2\mu_e$  was not considered as a new infection term. If it is considered to be so, then following the same procedure above, the expression of the basic reproduction number will be given by

$$\widehat{R}_0 = \frac{1}{2} \left( R_{hh} + \sqrt{R_{hh}^2 + 4R_{he}} \right).$$

However, it can be derived that the two expressions of the basic reproduction number have the same threshold as above, i.e.,  $R_0 > 1$  whenever  $R_{hh} + R_{he} > 1$ , which again confirm the importance of controlling all transmission routes. However, based on the values of the corresponding parameters, we will be able to determine the most significant transmission route. This will be shown in the following table, taking  $K = 0.5$ :

TABLE 2. Estimated values of the basic reproduction number

Transmission Route	Asymptomatic	Pre-symptomatic	Symptomatic	Total
$R_{hh}$	0.427	2.447	0.612	3.486
$R_{he}$	0.142	0.054	0.275	0.471
$R_0$	0.569	2.501	0.887	3.957
$\widehat{R}_0$	0.646	2.469	0.914	3.617

Clearly, the major contribution to the basic reproduction number comes from the direct pre-symptomatic transmission. Although the symptomatic individuals transmit large quantities of virus, for example via coughing but it is reasonable to think that the symptoms may urge the person to stay at home, wearing mask, limiting the number of contacts and hence this will reduce the transmission potential. On the other hand, individuals without symptoms are unaware of their infection risk to others and so they are likely to have more social interactions with others than those who have symptoms. Also, because of the delays in contact tracing and the nature of detection that focus on testing symptomatic persons, these findings could explain the greater proportion of pre-symptomatic transmission, see [6, 2, 7, 12, 17, 22].

**3.4. Sensitivity Analysis.** Here, we perform the normalized forward sensitivity index, also known as elasticity index, to explore the significant impact of the parameters of the model that are related to the basic reproduction number. It is defined as the relative change of  $R_0$  to the relative change in the parameter  $\phi$ , i.e.,

$$\Upsilon_{\phi}^{R_0} = \frac{\partial R_0}{\partial \phi} \frac{\phi}{R_0}.$$

Using the obtained explicit expressions of the basic reproduction number  $R_0$ , one can easily calculate the elasticity index with respect to each model parameter. The estimated values of the elasticity indices are obtained using the parameter values listed in Table 1. The obtained results are listed in Table 3.

TABLE 3. Sensitivity analysis of model (2)

Parameter ( $\phi$ )	$\Upsilon_{\phi}^{R_0}$	$\Upsilon_{\phi}^{\hat{R}_0}$
$\beta_1$	0.10801	0.11408
$\beta_2$	0.61844	0.65315
$\beta_3$	0.15464	0.16332
$\varepsilon_1$	-0.58102	-0.58568
$\varepsilon_2$	0.56110	0.58090
$\mu$	-0.00027	-0.00025
$\delta$	-0.08167	-0.06688
$\sigma$	-0.63190	-0.65713
$\gamma_1$	-0.14375	-0.12449
$\gamma_2$	-0.14252	-0.11671
$K$	-0.11891	-0.03472
$\alpha_1$	0.03577	0.01045
$\alpha_2$	0.06962	0.02033
$\beta_e$	0.11891	0.03472

In the above table, the sign of the elasticity index determines whether  $R_0$  increases (positive sign) or decreases (negative sign) with the parameter and the magnitude measures the relative

significant of the parameter. Clearly, the transmission rate of pre-symptomatic  $\beta_2$  has high positive index, while the reciprocal of infectious period before symptom onset  $\sigma$  has high negative index with  $R_0$ . From the obtained sensitivity results, pre-symptomatic plays a significant role in the spread of disease and can continue the outbreaks of COVID19 even though all symptomatic cases are isolated. Furthermore, the effectiveness of the control measures and prevention which focus on symptomatic transmission should be extended to pre-symptomatic and asymptomatic individuals. This can be achieved through social distancing, wearing face masks, maintaining personal hygiene, contact tracing to identify possible pre-symptomatic individuals and also isolation for pre-symptomatic individuals once identified in addition to symptomatic cases [12].

**3.5. Local and Global stability of DFE.** The local stability of the DFE can be established using Theorem 2 in [20] and hence, we have the following result:

**Lemma 3.5.1.** *The DFE of model 2, given by  $E_0$ , is locally asymptotically stable if  $R_0 < 1$  and unstable if  $R_0 > 1$ .*

The global stability of the DFE can be established using Lyapunov function described in [19]. This result is given in the following theorem:

**Theorem 3.1.** *If  $R_0 \leq 1$ , then the DFE of model (2) is globally asymptotically stable.*

*Proof.* First, consider the matrices  $F$  and  $V$  as given by (3) and (4), respectively. Then,  $V^{-1}$  is given by

$$V^{-1} = \begin{bmatrix} \frac{1}{\xi} & 0 & 0 & 0 & 0 \\ \frac{\lambda_1}{\xi(\mu + \gamma_1)} & \frac{1}{\mu + \gamma_1} & 0 & 0 & 0 \\ \frac{\lambda_2}{\xi(\mu + \sigma)} & 0 & \frac{1}{\mu + \sigma} & 0 & 0 \\ \frac{\lambda_2\sigma + \lambda_3(\mu + \sigma)}{\xi\eta(\mu + \sigma)} & 0 & \frac{\sigma}{\eta(\mu + \sigma)} & \frac{1}{\eta} & 0 \\ \frac{\alpha_1\lambda_1}{\xi(\mu + \gamma_1)} + \frac{\lambda_2}{\xi(\mu + \sigma)} + \frac{\alpha_2(\lambda_2\sigma + \lambda_3(\mu + \sigma))}{\xi\eta(\mu + \sigma)} & \frac{\alpha_1}{\mu + \gamma_1} & \frac{\eta + \sigma\alpha_2}{\eta(\mu + \sigma)} & \frac{\alpha_2}{\eta} & \frac{1}{\mu_e} \end{bmatrix}.$$

We clearly note that  $F \geq 0$  and  $V^{-1} \geq 0$ . Now, let  $x^T = (E, A, P, I, B)$  and  $y^T = (S, R)$ , then the disease compartments can be written as

$$x' = (F - V)x - f(x, y),$$

where  $f(x, y)$  is given by

$$f(x, y) = (F - V)x - \mathcal{F}(x, y) + \mathcal{V}(x, y)$$

$$= \begin{bmatrix} \beta_1 A \left(1 - \frac{S}{N}\right) + \beta_2 P \left(1 - \frac{S}{N}\right) + \beta_3 I \left(1 - \frac{S}{N}\right) + \frac{\beta_e B}{K(K+B)} (K(1-S) + B) \\ 0 \\ 0 \\ 0 \\ 0 \end{bmatrix}$$

Clearly,  $f(x, y) \geq 0$  since  $S \leq N \leq 1$ . Now, we construct Lyapunov function as described in Theorem 2.1 in [19] as follows

$$Q(t) = \omega^T V^{-1} x(t),$$

where  $\omega$  is the left eigenvector of the non-negative matrix  $V^{-1}F$  corresponding to the eigenvalue  $R_0 = \rho(V^{-1}F) = \rho(FV^{-1})$ . Computing  $\omega$ , we get

$$\omega^T = \left[ 0 \quad \frac{\beta_1 K}{\beta_e} \quad \frac{\beta_2 K}{\beta_e} \quad \frac{\beta_3 K}{\beta_e} \quad 1 \right].$$

Now, differentiating  $Q$  gives

$$\begin{aligned} Q' &= \omega^T V^{-1} x' \\ &= \omega^T V^{-1} (F - V)x - \omega^T V^{-1} f(x, y) \\ &\leq \omega^T (V^{-1}F - I_5)x \\ &= (R_0 - 1)\omega^T x \end{aligned}$$

where  $I_5$  is the identity matrix. Clearly,  $Q' \leq 0$  if  $R_0 < 1$ . Note that  $Q' = 0$  implies  $x = 0$  since  $f(0, y) = 0$ . When  $R_0 = 1$ ,  $Q' = 0$  implies  $f(x, y) = 0$ . In this case,  $f(x, y) = 0$  if and only if  $x = 0$ .

Hence,  $E_0$  is the largest invariant set in  $\Omega_0 = \{(S, E, A, P, I, R, B) \in \Omega, Q' = 0\}$ . Using LaSalle's invariance principle,  $E_0$  is an attractive point which leads to conclude that  $E_0$  is globally asymptotically stable provided that  $R_0 \leq 1$ .

**3.6. Existence of Endemic Equilibrium.** In this section, we show the existence of endemic equilibrium (EE). Let the EE of model (2) be given by

$$E_1 = (S^*, E^*, A^*, P^*, I^*, R^*, B^*),$$

and denote:

$$(5) \quad \Phi = \frac{\beta_1 A^*}{N^*} + \frac{\beta_2 P^*}{N^*} + \frac{\beta_3 I^*}{N^*} + \frac{\beta_e B^*}{K + B^*},$$

where  $N^* = \frac{1}{\mu}(\mu - \delta I^*)$ . Now, rewriting the components of the EE in terms of  $\Phi$ , we get

$$\begin{aligned} S^* &= \frac{\mu}{\Phi + \mu}, & E^* &= \frac{\Phi S^*}{\xi}, \\ A^* &= \frac{\lambda_1}{\mu + \gamma_1} E^*, & P^* &= \frac{\lambda_2}{\mu + \sigma} E^*, \\ I^* &= C_1 E^*, & B^* &= C_2 E^*, & R^* &= \frac{\gamma_1 A^* + \gamma_2 I^*}{\mu}, \end{aligned}$$

where,  $C_1 = \frac{\lambda_3(\mu + \sigma) + \sigma\lambda_2}{\eta(\mu + \sigma)}$  and  $C_2 = \frac{\lambda_1\alpha_1}{\mu + \gamma_1} + \frac{\lambda_2}{\mu + \sigma} + \frac{\alpha_2\lambda_3(\mu + \sigma) + \sigma\lambda_2}{\eta(\mu + \sigma)}$ .

Substituting the above expressions into equation (5), we have the following equation for  $\Phi$ :

$$a_1 \Phi^2 + a_2 \Phi + a_3 = 0$$

where

$$\begin{aligned} a_1 &= (K\xi + \mu C_2)(\xi - \delta C_1), \\ a_2 &= \mu K \xi^2 (1 - R_{hh} - R_{he}) + \mu^2 \xi C_2 (1 - R_{hh}) + \xi \mu K (\xi - \delta C_1) + \delta \beta_e C_1 C_2 \mu, \\ a_3 &= K \mu^2 \xi^2 (1 - R_{hh} - R_{he}). \end{aligned}$$

Obviously, the existence of EE follows immediately from the existence of positive solution of the above equation which can be determined using Descartes' rule of signs. Clearly,  $a_1$  is always positive since one can easily verify that  $\xi - \delta C_1 > 0$ . Hence, we consider the following cases:

- If  $R_0 \leq 1$ , then all coefficients are non-negative and so there is no positive solution.
- If  $R_0 > 1$ , then  $a_3 < 0$  which implies that a unique positive solution exists.

According to the above discussion, we conclude that EE of model (2) exists if  $R_0 > 1$ .

**3.7. Local stability of EE.** This section is devoted for local stability of EE. The result is stated in the following theorem:

**Theorem 3.2.** *The EE of model (2) is locally asymptotically stable if  $R_0 > 1$ .*

*Proof.* We use the results of Theorem 4.1 in [3] which is based on center manifold theory. We choose  $\beta_2$  to be a bifurcation parameter with a bifurcation value given by:

$$\beta_2^* = \frac{1}{K\lambda_2\eta(\mu + \gamma_1)} (K\xi\eta(\mu + \sigma)(\mu + \gamma_1) - \eta\lambda_1(\mu + \sigma)(\beta_1K + \beta_e\alpha_1) - \beta_e\eta\lambda_2(\mu + \gamma_1) - (\mu + \gamma_1)(\lambda_2\sigma + \lambda_3(\mu + \sigma)(\beta_3K + \beta_e\alpha_2))$$

which corresponds to  $R_0 = 1$ . Now, one can check that the Jacobian of model (2) at the DFE given by

$$J_{E_0, \beta_2^*} = \begin{bmatrix} -\mu & 0 & -\beta_1 & -\beta_2^* & -\beta_3 & 0 & -\frac{\beta_e}{K} \\ 0 & -\xi & \beta_1 & \beta_2^* & \beta_3 & 0 & \frac{\beta_e}{K} \\ 0 & \lambda_1 & -\mu - \gamma_1 & 0 & 0 & 0 & 0 \\ 0 & \lambda_2 & 0 & -\mu - \sigma & 0 & 0 & 0 \\ 0 & \lambda_3 & 0 & \sigma & -\eta & 0 & 0 \\ 0 & 0 & \gamma_1 & 0 & \gamma_2 & -\mu & 0 \\ 0 & 0 & \alpha_1\mu_e & \mu_e & \alpha_2\mu_e & 0 & -\mu_e \end{bmatrix}$$

has a simple zero eigenvalue. Then, computing the left eigenvector,  $v = [v_1 \ v_2 \ \cdots \ v_7]$ , associated with zero eigenvalue, we obtain

$$v_1 = v_6 = 0$$

$$v_2 = \frac{K\mu_e}{\beta_e} v_7$$

$$v_3 = \frac{\alpha_1\mu_e v_7 + \beta_1 v_2}{\mu + \gamma_1}$$

$$v_4 = \frac{\mu_e v_7 + \beta_2^* v_2 + \sigma v_5}{\mu + \sigma}$$

$$v_5 = \frac{\alpha_2\mu_e v_7 + \beta_3 v_2}{\eta}$$

$$v_7 = v_7 > 0.$$

and the right eigenvector,  $w = [w_1 \ w_2 \ \cdots \ w_7]^T$ , associated with zero eigenvalue is

$$w_1 = -\frac{\beta_1 w_3 + \beta_2^* w_4 + \beta_3 w_5 + \beta_e w_7 / K}{\mu}$$

$$w_2 = w_2 > 0$$

$$w_3 = \frac{\lambda_1 w_2}{\mu + \gamma_1}$$

$$w_4 = \frac{\lambda_2 w_2}{\mu + \sigma}$$

$$w_5 = \frac{\lambda_3 w_2 + \sigma w_4}{\eta}$$

$$w_6 = \frac{\gamma_1 w_3 + \gamma_2 w_5}{\mu}$$

$$w_7 = \alpha_1 w_3 + w_4 + \alpha_2 w_5$$

Let  $x = (S, E, A, P, I, R, B)$  and  $f_i$  ( $i = 1, 2, \dots, 7$ ) be the right hand side of the model (2). Then, calculating the values of  $a$  and  $b$  as defined in the above mentioned theorem, we get

$$\begin{aligned} a &= \frac{1}{2} \sum_{i,j,k=1}^7 v_i w_j w_k \frac{\partial^2 f_i(E_0, \beta_2^*)}{\partial x_j \partial x_k} \\ &= \frac{v_2}{K} \left( w_1 (\beta_1 w_3 + \beta_2^* w_4 + \beta_3 w_5 + \beta_e w_7) - \frac{w_7^2 \beta_e}{K} \right) < 0, \end{aligned}$$

since  $w_1 < 0$  and

$$b = \sum_{i,j=1}^7 v_i w_j \frac{\partial^2 f_i(E_0, \beta_2^*)}{\partial x_j \partial \beta_2} = \frac{K \mu_e \lambda_1}{\beta_e (\mu + \gamma_1)} w_2 v_7 > 0.$$

Hence, according to [3, 20], the EE is locally asymptotically stable if  $R_0 > 1$  and the system (2) undergoes forward bifurcation when  $\beta_2$  passes through bifurcation parameter  $\beta_2^*$ . The bifurcation diagram is given in Figure 2. MATCONT program is used to sketch this diagram [4].

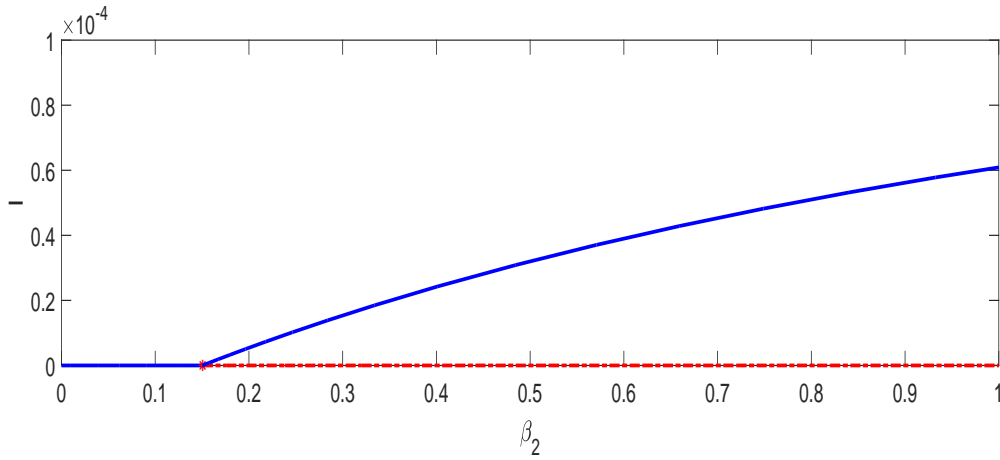


FIGURE 2. Bifurcation diagram with a bifurcation parameter  $\beta_2$ .

#### 4. NUMERICAL SIMULATION

In this section, we present some numerical simulations to illustrate the effect of the model parameters related to the pre-symptomatic transmission on the disease dynamics. The values of parameters are chosen as in Table 1. We begin with effect of pre-symptomatic transmission rate  $\beta_2$  and fixing other parameters as shown in Figure 3. Clearly, reducing the pre-symptomatic transmission rate  $\beta_2$  will decrease the peak number of symptomatic infected and also will delay the time to reach the peak. Hence, reducing the pre-symptomatic transmission will slow the



spread of COVID-19 and lead to flatten the curve of infected which prevents health care systems from being overrun and reduces the mortality due to the disease.

Figure 4 shows the effect of changing the portion of the symptomatic individuals who were pre-symptomatic  $\varepsilon_2$  before developing symptoms. It can be seen that increasing the fraction  $\varepsilon_2$  will lead to an increase in the peak number of symptomatic infected. Moreover, for large portion, there is a quick increase and also decline in the number of symptomatic infected as shown in the Figure. Figure 5 presents the effect of infectious period before symptom onset. We observe that increasing  $\sigma$  (reciprocal of infectious period) will decrease the maximum number of infected. In other words, for short period of infectiousness before symptom onset, the maximum number of symptomatic infected is less and the time to reach this maximum is delayed. All these results show the importance of identifying pre-symptomatic individuals in order to minimize their contribution to the disease transmission.

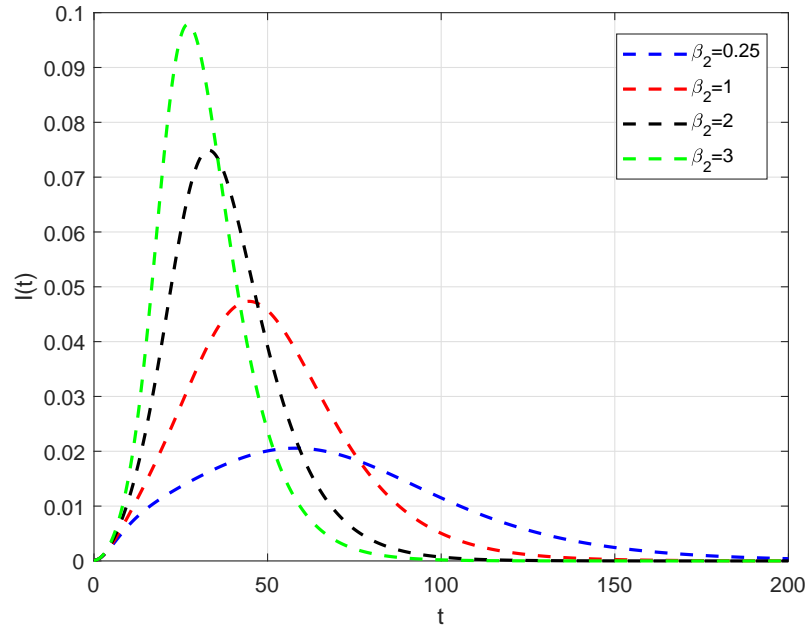


FIGURE 3. Effect of pre-symptomatic transmission rate  $\beta_2$  with  $\beta_1 = 0.125, \beta_3 = 0.12875$ .

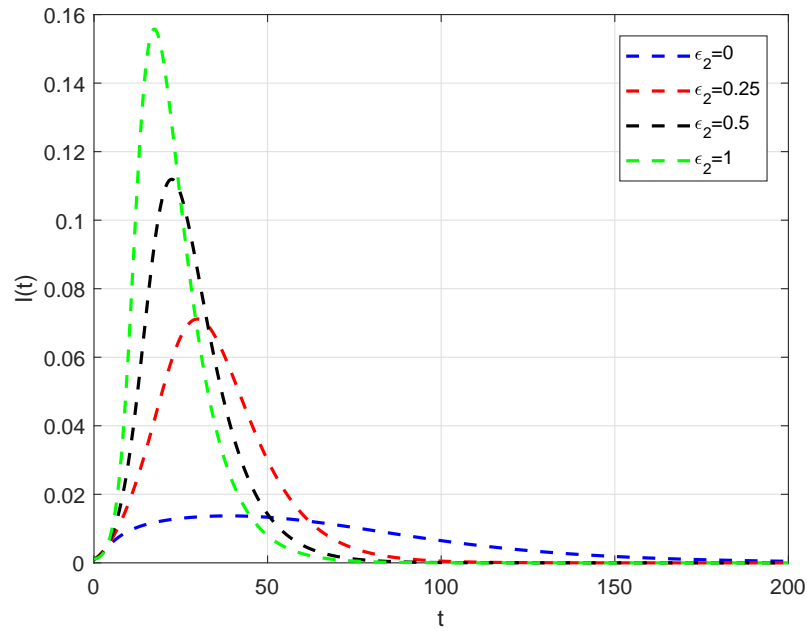


FIGURE 4. Effect of the portion of symptomatic individuals who started as pre-symptomatic  $\epsilon_2$ .

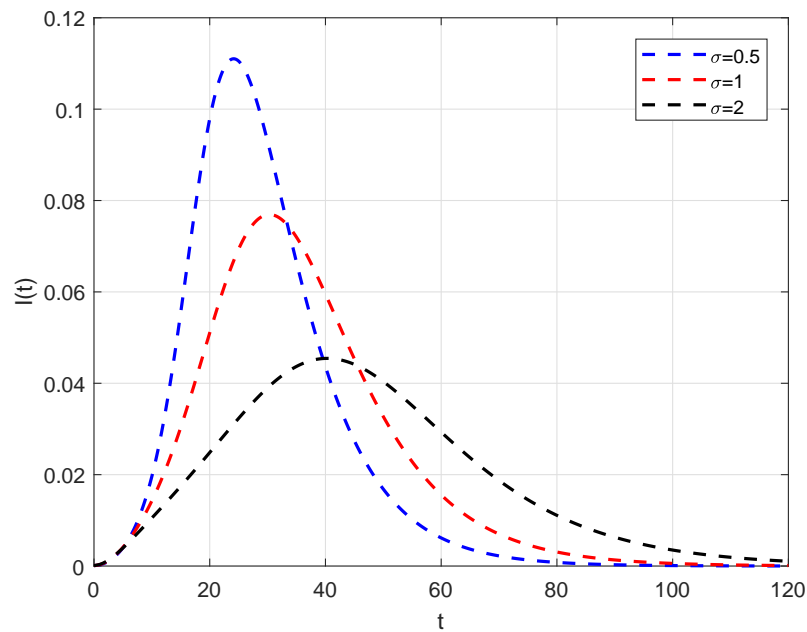


FIGURE 5. Effect of infectious period before symptom onset.

## 5. CONCLUSION

A mathematical model has been proposed to investigate the hidden role of pre-symptomatic transmission in COVID-19 dynamics. The model includes the three main routes of transmission, namely, asymptomatic, pre-symptomatic and symptomatic transmissions in the forms of direct (human to human) and indirect (environment to human) transmissions. The model has been first normalized using a set of normalized variables and the normalized model has been then fully analyzed both qualitatively and quantitatively. The analysis started by defining a bounded invariant region where the model has a biological sense. The basic reproduction number was then calculated using the next generation method. The obtained expressions include contributions from direct and indirect asymptomatic, pre-symptomatic and symptomatic transmissions. The estimated values of the basic reproduction number show that the major contribution is coming from direct pre-symptomatic transmission. Sensitivity analysis has been then carried out to identify the parameters with high impact on the basic reproduction number and hence on the disease transmission. It has been found that two parameters related to pre-symptomatic transmission have the highest impact on the basic reproduction number, namely, the pre-symptomatic transmission rate with positive impact and the rate at which pre-symptomatic individuals become symptomatic with negative impact. The later implies that the longer infectious individuals stay as pre-symptomatic the higher they contribute to the disease transmission. Stability of equilibrium points has been also addressed. It has been shown that the disease free equilibrium is globally asymptotically stable whenever the basic reproduction number is less than unity and the endemic equilibrium point is locally asymptotically stable whenever the basic reproduction number is greater than unity. Finally, the obtained theoretical results have been demonstrated numerically. In particular, numerical simulations have been carried out to illustrate the effect of some model parameters related to pre-symptomatic transmission on COVID-19 transmission dynamics, namely, the pre-symptomatic transmission rate, the portion of symptomatic individuals who started as pre-symptomatic and the rate at which the pre-symptomatic individuals become symptomatic. The obtained results were demonstrated

graphically and showed that all these parameters have the effect of reducing the maximum number of symptomatic individuals and delaying the time it takes to reach the maximum. In conclusion, it is very important to adopt strategies to identify the pre-symptomatic individuals as early as possible, such as contact tracing, in order to minimize their contribution to the disease transmission.

### CONFLICT OF INTERESTS

The author(s) declare that there is no conflict of interests.

### REFERENCES

- [1] J. B. Aguilar, J.S. Faust, L. M. Westafer, J.B. Gutierrez, Investigating the impact of asymptomatic carriers on COVID-19 transmission, medRxiv. doi: <https://doi.org/10.1101/2020.03.18.20037994>. (2020).
- [2] M. Casey, J. Griffin, C. G. McAloon, A. W. Byrne, J. M. Madden, D. McEvoy, A. B. Collins, K. Hunt, A. Barber, F. Butler and others, Estimating pre-symptomatic transmission of COVID-19: a secondary analysis using published data, medRxiv. doi: <https://doi.org/10.1101/2020.05.08.20094870>. (2020).
- [3] C. Castillo-Chavez, B. Song, Dynamical models of tuberculosis and their applications, *Math. Biosci. Eng.* 1 (2004), 361-404.
- [4] A. Dhooge, W. Govaerts, Y. A. Kuznetsov, H. G. Meijer, B. Sautois, New features of the software MatCont for bifurcation analysis of dynamical systems, *Math. Comput. Model. Dyn. Syst.* 14 (2008), 147–175.
- [5] I. ELmojtaba, F. Al-Musalhi, Fatma, A. Al-Ghassani, N. Al-Salti, Investigating the Role of Environmental Transmission in COVID-19 Dynamics: A Mathematical Model Based Study, *Research Square*. doi: <https://doi.org/10.21203/rs.3.rs-32476/v1>. (2020).
- [6] Imperial College London, Whole-town study reveals more than 40% of COVID-19 infections had no symptoms, *ScienceDaily* (2020), [www.sciencedaily.com/releases/2020/06/200630103557.htm](http://www.sciencedaily.com/releases/2020/06/200630103557.htm).
- [7] L. Ferretti, C. Wymant, M. Kendall, L. Zhao, A. Nurtay, L. Abeler-Dörner, M. Parker, D. Bonsall, C. Fraser, Quantifying SARS-CoV-2 transmission suggests epidemic control with digital contact tracing, *Science* 368 (2020), eabb6936.
- [8] M. Gatto, E. Bertuzzo, L. Mari, S. Miccoli, L. Carraro, R. Casagrandi, A. Rinaldo, Spread and dynamics of the COVID-19 epidemic in Italy: Effects of emergency containment measures, *Proc. Nat. Acad. Sci.* 117 (2020), 10484–10491.
- [9] X. He, E.H.Y. Lau, P. Wu, et al. Temporal dynamics in viral shedding and transmissibility of COVID-19, *Nat. Med.* 26 (2020), 672–675.

- [10] A. Kimball, K. M. Hatfield, M. Arons, et al. Asymptomatic and presymptomatic SARS-CoV-2 infections in residents of a long-term care skilled nursing facility-King County, Washington, March 2020, *Morb. Mortal. Wkly. Rep.* 69 (2020),377-381.
- [11] E. Lavezzo, E. Franchin, C. Ciavarella, et al. Suppression of a SARS-CoV-2 outbreak in the Italian municipality of Vo', *Nature* 584 (2020), 425-429.
- [12] S. M. Moghadas, M.C. Fitzpatrick, P. Sah, A. Pandey, A. Shoukat, B. H. Singer, A. P. Galvani, The implications of silent transmission for the control of COVID-19 outbreaks, *Proc. Nat.Acad. Sci.* 117 (2020), 17513-17515.
- [13] R.K. Mohapatra, L. Pintilie, V. Kandi, A.K. Sarangi, D. Das, R. Sahu, L. Perekhoda, The recent challenges of highly contagious COVID-19, causing respiratory infections: Symptoms, diagnosis, transmission, possible vaccines, animal models, and immunotherapy, *Chem Biol Drug Des.* (2020) cbdd.13761. <https://doi.org/10.1111/cbdd.13761>.
- [14] S. Mwalili, M. Kimathi, V. Ojiambo, D. Gathungu, R. Mbogo, SEIR model for COVID-19 dynamics incorporating the environment and social distancing, *BMC Res. Notes.* 13 (2020), 352.
- [15] H. Nishiura, N.M. Linton, A.R. Akhmetzhanov, Serial interval of novel coronavirus (COVID-19) infections, *Int. J. Infect. Dis.* 93 (2020), 284-286.
- [16] V. N. Ojiambo, M. Kimathi, S. Mwalili, D. Gathungu, R. Mbogo, A Human-Pathogen SEIR-P Model for COVID-19 Outbreak under different intervention scenarios in Kenya, *medRxiv.* doi: <https://doi.org/10.1101/2020.05.15.20102954> (2020).
- [17] D.P. Oran, E.J. Topol, Prevalence of Asymptomatic SARS-CoV-2 Infection: A Narrative Review, *Ann. Intern. Med.* 173 (2020), 362–367.
- [18] A. Senapati, S. Rana, T. Das, J. Chattopadhyay, Impact of intervention on the spread of COVID-19 in India: A model based study, *ArXiv:2004.04950 [Math, q-Bio].* (2020).
- [19] Z. Shuai, P. van den Driessche, Global stability of infectious disease models using Lyapunov functions, *J. Appl. Math.* 73 (2013), 1513–1532.
- [20] P. Van den Driessche, J. Watmough, Reproduction numbers and sub-threshold endemic equilibria for compartmental models of disease transmission, *Math. Biosci.* 180 (2002), 29-48.
- [21] J. Wang, Mathematical models for COVID-19: applications, limitations, and potentials, *J. Public Health Emerg.* 4 (2020), 9.
- [22] W. E. Wei, Z. Li, C. J. Chiew, Calvin, S. E. Yong, M. P. Toh, V. J. Lee, Presymptomatic Transmission of SARS-CoV-2 in Singapore, January 23–March 16, 2020. *Morb. Mortal. Wkly. Rep.* 69(2020), 411-415.
- [23] World Health Organization Coronavirus disease 2019 (COVID-19): situation report 72, (2020).
- [24] C. Yang, J. Wang, A mathematical model for the novel coronavirus epidemic in Wuhan, China, *Math. Biosci. Eng.* 17 (2020), 2708–2724.

- [25] W. Zhang, Z. Weituo, Estimating the presymptomatic transmission of COVID19 using incubation period and serial interval data, medRxiv. doi: <https://doi.org/10.1101/2020.04.02.20051318> (2020).